

Department of Physics and Astronomy
Experimental Particle Physics Group
Kelvin Building, University of Glasgow,
Glasgow, G12 8QQ, Scotland
Telephone: +44 (0)141 330 2000 Fax: +44 (0)141 330 5881

Evaluation of Silicon Monolithic APS as a Neutron Detector

Dzmitry Maneuski¹, Lars Eklund¹, Miloslav Kralik²,
Andrew Laing¹, Val O'Shea¹, Stanislav Pospisil³,
Zdenek Vykydal³

¹ University of Glasgow, Glasgow, G12 8QQ, Scotland

² Czech Metrology Institute, Prague, Czech Republic

³ Institute of Experimental and Applied Physics, Czech Technical University, Prague, Czech Republic

Abstract

Progress in the development of neutron imaging facilities requires more sophisticated and advanced tools for high resolution and efficient neutron detection. This paper reports on the evaluation of CMOS Monolithic Active Pixel Sensor (MAPS) technology as a neutron detector. The sensor HEPAPS4, which was originally designed for high energy physics applications, was coated with two types of conversion material. The ${}^6\text{LiF}$ converter is suitable for the detecting thermal neutrons, while the polyethylene converter is used for the tracking fast neutrons. The results showed that such a technology is suitable for the detection of both fast and thermal neutrons.

IEEE, Nuclear Science Symposium
19 - 25 October 2008, Dresden, Germany

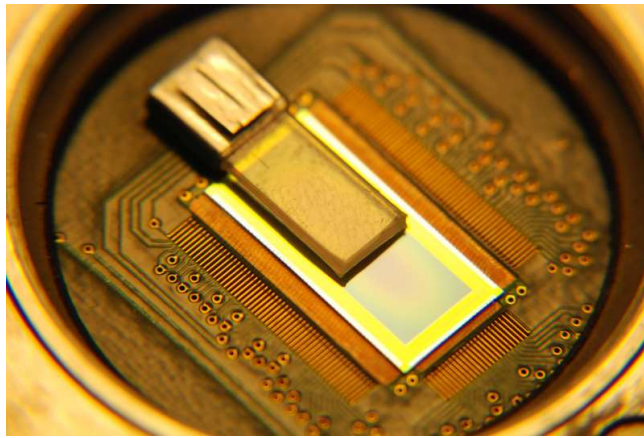


Figure 1: The HEPAPS4 sensor with the polyethylene converter

1 Introduction

Neutron imaging is a fast growing and powerful technique for non-destructive testing with unique features compared to roentgenography and other methods. The advantages include higher sensitivity to materials with a lower atomic number (e.g. hydrogen and carbon) and deeper penetration of thick objects made of heavy elements (e.g. lead and bismuth). Conventional tools, for example image plates for neutron radiography, show good results, however, there are many limitations. New imagers require higher performance parameters, especially with respect to more sophisticated functionality, time resolution, dynamic range and other properties. CMOS MAPS technology has already demonstrated several advantages over other existing technologies in particle tracking, imaging and radiation detection applications, with respect to functionality, power consumption, readout speed and fabrication costs. In this paper we suggest that CMOS MAPSs, if covered with an appropriate conversion material, are suitable for both thermal and fast neutron detection.

2 Materials and methods

2.1 The HEPAPS4 sensor

The HEPAPS4 [1] is a large area device (384×1024 pixels at $15 \mu\text{m}$ pitch) designed for high energy physics applications at Rutherford Appleton Laboratory. The sensor features a standard three nMOS design with enclosed geometry transistor pixel architecture (EGT) [2]. Charged particles induce charge in the field oxide layer of the transistor which leads to a source to drain leakage current in conventional transistor designs. EGT gives improved radiation tolerance. The in-pixel circuitry is implemented in a p-well with one $1.7 \times 1.7 \mu\text{m}^2$ diode. Charge deposited in the sensor is collected from the $20 \mu\text{m}$ thick p-type epi-layer. The sensor is read out by addressing pairs of rows and sampling their signals on the capacitors at the end of each column. The readout cycle loops through these capacitors and multiplexes their voltages on four differential outputs where they are digitised using 14-bit off chip ADC. The read-out system for the HEPAPS4 has a 33 MHz clock and features configurable current and voltage biases as well as a variable integration time and a region of interest (ROI) readout. The sensor performance is described in detail in Ref. [3].

2.2 Neutron converters

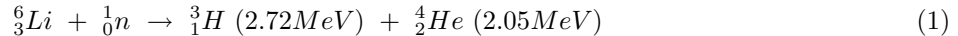
The adaptation of the sensor for neutron detection corresponds to the design given in [4], [5]. Two HEPAPS4 sensors were covered with different neutron converters. Approximately half of each sensor was left bare in order to quantify direct detection efficiency in silicon.

2.2.1 Fast neutron converter (Polyethylene)

Hydrogen enriched material was of prime interest as an efficient fast neutron moderator. A 1.1 mm thick polyethylene (PE) converter was put on top of the sensor (Fig. 1). As a result of neutron interaction in PE, a recoiled proton is produced by an elastic neutron scattering on hydrogen, which can be detected by the sensor.

2.2.2 Thermal neutron converter (${}^6\text{Li}$)

${}^6\text{Li}$ based converter, in the form of fine ${}^6\text{LiF}$ powder (enrichment 89%, density $\sim 2 - 3 \text{ mg/cm}^2$) mixed with polyvinyl alcohol as a binder (less than 5% of weight), was deposited on thin aluminium foil and put in close contact with the sensor surface. The interaction is as follows:



the products are oppositely directed at sufficiently small neutron energies. Both α -particles and tritium can be detected by the HEPAPS4 sensor.

2.3 Experimental setup

The measurements were performed at the Czech Metrology Institute in Prague using three neutron sources (two for fast neutrons and one for thermal neutrons). Thermal neutrons were generated by a fission reaction in a natural source and moderated by graphite to an average energy of 0.025 eV . The sensor with the converter was placed on top of the opened reactor cavity.

Fast neutrons from ${}^{252}\text{Cf}$ (2 MeV mean energy) and ${}^{241}\text{AmBe}$ (4 MeV mean energy) were used. The sources were placed at a distance of 5 and 10 cm respectively in order to obtain a balance between the interaction occupancies of the detector and reasonable statistics.

3 Results

The response of the sensor to thermal neutrons is depicted in Fig. 2. Area 1 indicates typical sensor response to either α -particle or tritium nucleus, while area 2 indicates ghost events which are the result of image lag due to the fact that the sensor can operate only in soft reset mode¹.

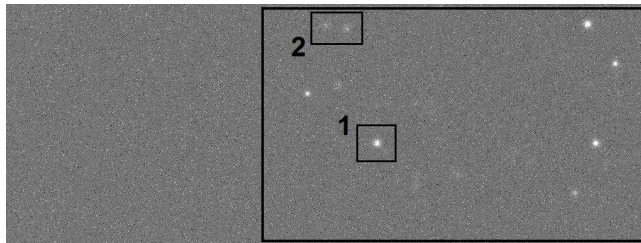


Figure 2: Sensor response to thermal neutron. Right half of the area is covered with the ${}^6\text{LiF}$ converter.

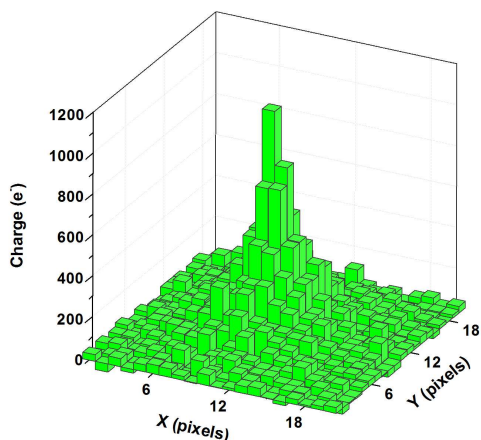


Figure 3: Typical cluster response to tritium interaction in the sensor.

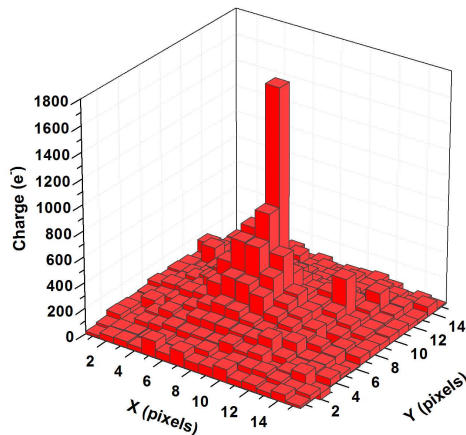


Figure 4: Bragg peak cluster resulting from particle energy deposition within epi-layer of the sensor.

¹)Soft reset results in a reset noise lowered by a factor $\sqrt{2}$. However, frames taken utilising soft reset are affected by image lag, where an artifact from a previous frame is superimposed on the current image.

Before signal frames were acquired, a set of dark frames were taken and pedestal was calculated for each pixel. The pedestal was then subtracted from each signal frame. A cluster analysis algorithm²⁾ was developed in order to understand the sensor response to the secondary particles created. A typical symmetrical tritium cluster is depicted in Fig. 3 and is ~ 7 pixels in diameter. Some secondary particles enter the sensor at acute angles and lose all their energy in the epi-layer. The response to such a particle is depicted in Fig. 4 and follows a Bragg distribution.

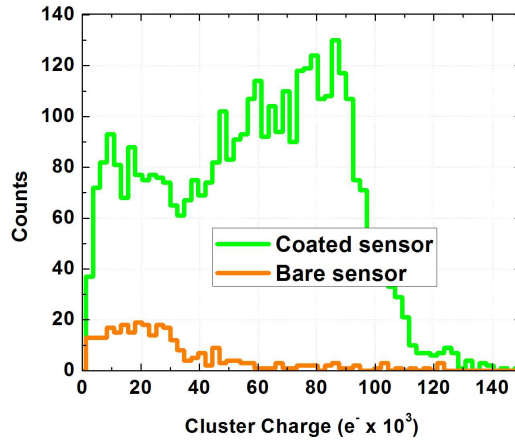


Figure 5: Cluster charge distribution as a result of thermal neutron interaction in the ${}^6\text{LiF}$ converter as well as in bare sensor.

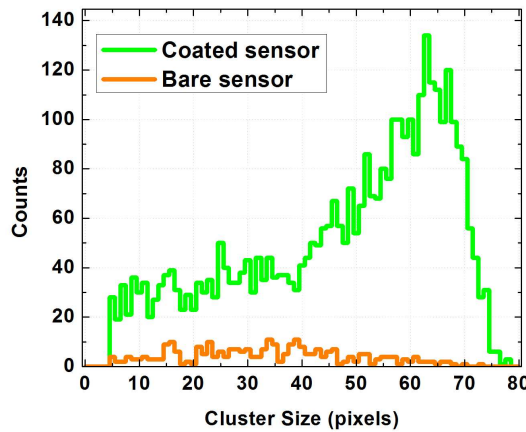


Figure 6: Thermal neutron response cluster size distribution.

3.1 Thermal neutron response

The cluster charge distribution depicted in Fig. 5 suggests that both α -particles and tritium contribute to the signal. Two energy peaks can be identified. It is assumed that the higher-energy peak corresponds to ${}^3\text{H}$, while the other is due to α -particles. Such a spectrum could be the result of the overlapping of the Bragg curve from the tritium interaction in the epi-layer of the sensor with the end of the Bragg peak from the α -particle. A 2.72 MeV triton can travel up to $30\ \mu\text{m}$ in silicon [7]. Taking into account that nearly right angle events are rare, one can assume that most of the charge is collected in the epi-layer or diffused back from the adjoining bulk volume. A 2.05 MeV α -particle, even if it enters the sensor at a right angle, will lose most of its energy in the converter, passivation layer and electronics ($\sim 6\ \mu\text{m}$ in total). Fig. 5 reflects the spectrum from thick ${}^6\text{LiF}$ converter and a silicon diode [8].

²⁾The cluster analysis algorithm is based on identifying isolated seed hits. A hit is considered as such if it is the highest significance

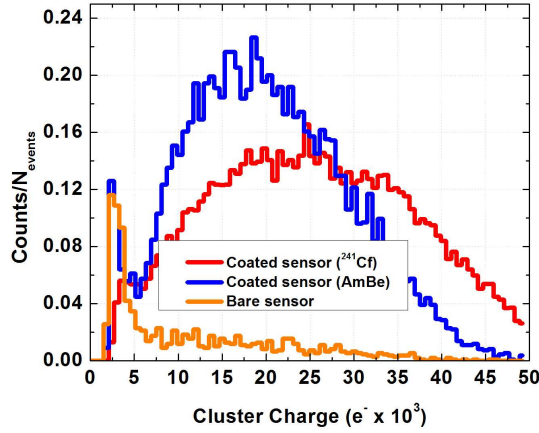


Figure 7: Sensor cluster charge response to fast neutrons in a PE converter and in silicon.

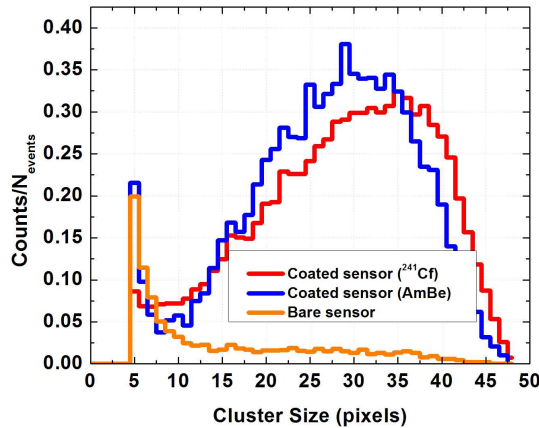


Figure 8: Cluster size distribution for fast neutron interactions.

3.2 Fast neutron response

Fig. 7 and Fig. 8 show cluster charge and cluster size distributions respectively, normalised to the total number of events recorded for ^{252}Cf (~ 32000) and $^{241}\text{AmBe}$ (~ 10000). The range of the recoiled proton ($\sim 1-4\text{ MeV}$) in silicon is $\sim 90-110\ \mu\text{m}$ [7]. The geometry of the setup and kinematics of fast neutron interactions suggest that only a few protons (which enter the sensor at very acute angles) can deposit all their energy in the epi-layer. The energy loss of the recoiled protons are on average higher for ^{252}Cf because of the lower average kinetic energy of neutrons.

3.3 Direct silicon interactions

Both fast and thermal neutrons can interact directly with silicon via elastic and inelastic $\text{Si}(n,p)$ and $\text{Si}(n,\alpha)$ scattering reactions. The cluster analysis was carried out in the region which was not covered with the converter in order to study these phenomena. The results from both fast and slow neutrons show that $\sim 10\%$ of all neutron interactions consist of the reactions in silicon. This has to be taken into account when the overall detection efficiency is calculated.

Fig. 5 shows that $\sim 50\%$ of charge deposited in the lower-energy end of the spectrum comes from the silicon interaction. This illustrates the idea that only α -particles entering the sensor at roughly right angles reach the epi-layer of the sensor.

Products of neutron reactions in silicon are shown for all ranges of cluster sizes identified (Fig. 6 and Fig.

pixel passing a $10 \times \sigma_{noise}$ cut is a 5×5 region, which is surrounded only by pixels not passing the cut in a larger 11×11 region.

8) with the highest contribution from fast neutrons products occurring in clusters of 4 - 10 pixels in size. This can be seen in the Fig. 8 for both ^{252}Cf and $^{241}\text{AmBe}$ where bare and coated part of the sensor are compared.

3.4 Detection efficiency

Table 1 summarises detection efficiencies for both direct silicon interactions and via proton generation in the PE converter. The detection efficiency for thermal neutrons cannot be calculated due to inaccurately known neutron flux at the top of the graphite prism cavity where the sensor was placed. However following [4] and [5], thermal neutron detection efficiency is estimated to be 3 - 5 %.

Table 1: HEPAPS4 fast neutron detection efficiency

	PE converter (%)	Silicon reaction (%)
$^{241}\text{AmBe}$	$(6 \pm 2) \times 10^{-2}$	$(0.15 \pm 0.05) \times 10^{-2}$
^{252}Cf	$(3 \pm 1) \times 10^{-2}$	$(0.50 \pm 0.15) \times 10^{-2}$

4 Discussion

Recent advances in the development of CMOS APS as well as increased interest in the use of neutrons for material study [4], [9] give confidence that such a technology, combined with relatively uncomplicated post processing, will open a broad range of applications. This could include online beam diagnostics and monitoring at neutron scattering facilities. The tremendous flexibility of design options and standard CMOS fabrication processes allow task specific functionality integration on chip at no significant extra cost. Industrial quality control, security equipment and medical imaging also contribute to a long list of possible future applications for CMOS MAPSs as neutron detection systems.

5 Conclusions

We have successfully demonstrated that CMOS MAPSs, if covered with the appropriate conversion material, are suitable for γ -transparent fast and thermal neutron detection. The calculated conversion efficiency for fast neutrons is similar to hybrid pixel detector technology ($\sim 0.1\%$)[6]. Further irradiation experiments together with extensive simulations will be carried out in order to fully understand the spectra and performance capabilities. The results obtained pave the way to investigate an opportunity for a number of applications utilising all the advantages of the MAPS technology.

6 Acknowledgement

The authors thank K. Mathieson and R. Bates from the University of Glasgow for comments on the manuscript.

References

- [1] L. Eklund *et al.*, First results from the HEPAPS4 Active Pixel Sensor, NIM A, in press.
- [2] D. G. Mavis *et al.*, Employing radiation hardness by design techniques with commercial integrated circuit processes, Proceedings of Digital Avionics Systems Conference, 1997, pp. 2.1-152.1-22.
- [3] D. Maneuski *et al.*, Characterisation of HEPAPS4 - a family of CMOS active pixel sensors for charged particle detection, PSD8 proceedings.
- [4] J. Jakubek *et al.*, Spatial resolution of Medipix-2 device as neutron pixel detector, NIM A, **546**, Issues 1-2, 1 July 2005, Pages 164-169.
- [5] Z. Vykydal *et al.*, The Medipix2-based network for measurement of spectral characteristics and composition of radiation in ATLAS detector, IWoRID 2008 proceedings, to be published.
- [6] D. Greiffenberg *et al.*, Detection efficiency of ATLAS-Medipix detectors with respect to neutrons, IWoRID 2008 proceedings, to be published.

- [7] D. J. Skyrme, *The passage of charged particles through silicon*, NIM, **57**, 1967, pages 61-73
- [8] S. Pospisil *et al.*, *Si diode as a small detector of slow neutrons*, Radiation Protection Dosimetry, **Vol. 46**, No. 2, pages 115-118 (1993).
- [9] M. W. Johnson, *Silicon APS detectors for neutron scattering*, NIM A, **501**, 2003, pages 72-79